

Design Optimization of Sludge Hygenization Research Irradiator

Ajit Kumar Mahendra*, Sashi Kumar G.N., Ashis Sanyal,
G. Gouthaman and T.K. Bera

Chemical Technology Group, Bhabha Atomic Research Centre,
Trombay, Mumbai, 400094, India.

*e-mail: mahendra@barc.gov.in

ABSTRACT

The paper addresses the design optimization of the radiation chamber of Sludge Hygenization Research Irradiator (SHRI). The distribution and placement of source assembly are the parameters of optimization. The physical parameters that are associated with radiation effects are the absorbed dose rate, the dose distribution and radiation quality. The objective of the present study is to achieve increased average absorbed dose rate with improved distribution by minimal alteration in the geometry of the existing SHRI that was designed by the Bhabha Atomic Research Centre and installed in Vadodara, India. A new approach is proposed to evaluate the time averaged absorbed dose rate and is validated. A better design for the arrangement of source assembly inside the irradiator vessel of SHRI has been proposed.

Keywords: SHRI, computational fluid dynamics, design optimization, cylindrical shell source, time averaged absorbed dose rate

Nomenclature

- ^{60}Co = radioactive Cobalt isotope with atomic mass of 60.
 ^{137}Cs = radioactive Cesium isotope with atomic mass of 137.
 C_{flux} = flux to dose rate conversion factor, conversion factor depends on the emitted gamma radiation, absorption coefficient of the medium, etc.
 d = diameter of the source rod
 D_i = net absorbed dose, Gy
 \dot{D}_p = absorbed dose rate at a point p , Gy/hr
 \dot{D}_t = time averaged absorbed dose rate for the whole domain, Gy/hr
 \dot{D}_v = volume averaged absorbed dose rate for the whole domain, Gy/hr
 Gy = Gray, absorbed dose
 H = half of the height of the cylindrical source rods
 kCi = kilo Curie, unit of radiation source strength, ($1PBq = 27.03 kCi$)
 l = length of the path traveled by a fluid particle
 N = total number of elements in the computational domain
 PBq = Peta Becquerel, unit of radiation source strength,
 ($1Bq = 1$ atom disintegration /second)
 r_d = distance from center of source rod
 r_s = radius of cylindrical source rods
 S_o = source strength, in kCi/m^2
 v = velocity of fluid
 V = volume of fluid
 θ_c = critical angle above which source surface is not visible.
 τ = time taken by a particle along a streamline

1. INTRODUCTION

The treatment of sewage sludge using gamma ray radiation facility was first built in 1973 at Geiselbullach, West Germany. Since then many other countries like USA, India, Japan, Austria, Russia, Canada, Poland and Argentina have constructed sludge irradiators and demonstrated the process [1, 2].

They either use i) gamma ray irradiation using ^{60}Co or ^{137}Cs or ii) electron beam accelerator irradiation source.

The residue left over after effluent treatment of municipal wastewater is referred to as sewage sludge. Sewage sludge contains useful plant nutrients and has properties that makes it a good soil conditioner. However, it also contains pathogenic bacteria, viruses, protozoa, parasites and other microorganisms that can cause disease. Surface disposal or agricultural use of untreated sewage sludge can create a potential for human exposure to these organisms through direct and indirect contact. Many countries have regulations for the use and disposal of sewage sludge in order to protect public health from these organisms.

There are many processes to reduce pathogen level in the sewage sludge: i) composting using windrow method at $55\text{ }^\circ\text{C}$, ii) heat drying with hot gases about $80\text{ }^\circ\text{C}$, iii) heating the liquid sewage to high temperatures around $180\text{ }^\circ\text{C}$, iv) thermophilic aerobic digestion at $55\text{ }^\circ\text{C}$ to $60\text{ }^\circ\text{C}$, v) beta ray irradiation at room temperature, vi) gamma ray irradiation at room temperature, etc. to mention a few.

The pathogen reduction requirements for sewage sludge are divided into two categories: Class A and Class B [3]. The implicit goal of the Class A requirements is to reduce the pathogens in sewage sludge so that its immediate use for agricultural farms is possible. The implicit goal of the Class B requirements is to reduce pathogens in sewage sludge to levels that are unlikely to pose a threat to public health and the environment when used in seclusion. The density of fecal coliform in the sewage sludge should be less than 1,000 most probable number per gram total solids (dry weight basis) after irradiation. Then it conforms to a Class A reduction process.

The appropriately treated sewage sludge has vast potential in agriculture as i) a soil conditioner, ii) in improving the efficiency of chemical fertilizers and iii) to a small scale as supplementary animal feed. In tropical countries like India high temperature and humidity accelerates the growth of bacteria in soil. The bacteria deplete the soil of its organic content. The treated and dried sewage sludge forms a good soil conditioner to upgrade the soil organic content. An optimum ratio of chemical fertilizers with sludge forms a good product for agricultural application, which retains the usefulness of both ingredients.

One of the primary concerns for sewage sludge irradiator design is the regrowth of pathogenic coliform. One needs to completely eliminate bacteria through treatment, since some of them can regrow very rapidly. Viruses, helminths, and protozoa cannot regrow once reduced by the treatment. The irradiation is aimed at reducing the bacteria by 6 to 7 log scales and viruses by at least one log scale. Also, the reduction of pathogens should be uniform throughout the sludge. This can be achieved by having uniformity in the absorbed dose of the sewage sludge.

The present study involves the gamma ray irradiation facility in India, which was built and commissioned by Bhabha Atomic Research Centre. It was named as Sludge Hygenization Research Irradiator (SHRI) facility and is situated at Vadodara in India. Figure 1 schematically depicts the said SHRI plant whose main purpose is the treatment of municipal sewage. Irradiation of the sewage

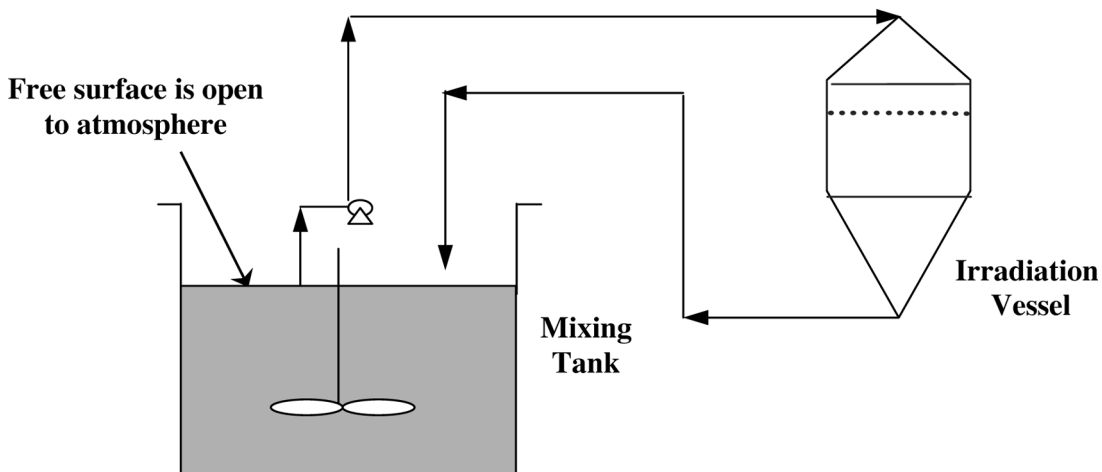


Figure 1. Schematic of the irradiation process at SHRI.

sludge by a gamma source (^{60}Co) has been carried out to reduce the microbial load by several log cycles as reported by Iya *et al.* [4], Krishnamurthy [5] and Lavale *et al.*, [6]. The processed sludge after drying turns into a safe fertilizer. Having benefited from this plant for many years, a few more such installations have been planned in the country. Benny *et al.* [7, 8] have measured the absorbed dose rate on sand particles using thermoluminescence (TL) dosimetry in SHRI. Pant *et al.* [9] have performed tracer studies in the existing design to determine the dead volume in the irradiator. Mahendra *et al.* [10] studied the operational optimization of SHRI. The present paper addresses the issue of improving i) the absorbed dose rate and ii) the uniformity of absorbed dose in the sewage sludge.

Section 2 discusses the existing SHRI configuration. Section 3 discusses the method of determining the average absorbed dose rate from cylinder source of finite length, followed by the validation of scheme used for SHRI. Section 4 elaborates various design configurations considered for analysis, which is followed by discussion of results in section 5. Conclusions are finally given in section 6.

2. EXISTING DESIGN OF SHRI

The process equipment consists of primarily an irradiator vessel and a mixing tank as shown in Fig. 1. The irradiator consists of a stainless steel vessel of 3.7 m^3 volume. In order to distribute the sludge uniformly across the cross-section of the vessel, a conical shaped distributor is mounted at the top of the vessel. The sludge is maintained at a level below the distributor. At any point of time the irradiator is loaded with a volume of 3 m^3 of sludge. There is a free surface of the loaded sludge below the distributor and about 390 mm above the source rods. A planar grid source assembly consisting of 13 tubes is present in the irradiator as shown in Fig.2. Each of these tubes is loaded with 2 source pencils and together all the 13 tubes can have maximum capacity of 18.5 PBq (550 kCi). The validation and optimization studies are carried out for the irradiator with a source of strength of 2.78 PBq (75.135 kCi). After irradiation the sludge is passed to a mixing tank. This open air-mixing tank of 12 m^3 enables availability of oxygen and helps in radiation fixation thereby improving the G-value. The G-value measures the amount of species involved in the irradiation treatment per unit of radiation energy absorbed by the material. Ionizing radiation interacts with water inducing a reduction in chemical and biochemical oxygen demand. Sufficient residence time inside the mixing tank is maintained so as to complete the radiation fixation. The sludge is then pumped back to the irradiator in a closed circulation loop. This circulation also aids in achieving uniform exposure to gamma radiation. The sludge containing 2 to 6% solids by weight has a bulk density around 1010 to 1050 kg/m^3 . In order to avoid settling of the solids inside the irradiator a pumping rate between 20 and $60 \text{ m}^3/\text{hr}$ is maintained [9]. A value of $32 \text{ m}^3/\text{hr}$ has been assumed for analysis in this paper. Also the bottom portion of the irradiator is in form of a reducer which helps to avoid settling of sludge.

The irradiator operates in a batch process and the contents after circulating for a predetermined amount of time are drained into drying beds for subsequent use as fertilizer. The time of circulation should be such that the coliform counts are below $10^2/\text{ml}$ (in the sludge) after irradiation. A minimum absorbed dose of $3 - 4 \text{ kGy}$ (Suess [11]) should be assured uniformly in the sludge. This dosage assures that no regrowth of coliform takes place in the post-irradiated sludge. This dosage of $3-4 \text{ kGy}$ can achieve a pathogen reduction factor of $10^6 - 10^7$ bacterial and 10^1 of viruses [6].

The radiation effects can be associated with physical and environmental factors. The chemical changes associated are measured in terms of G-value. The physical parameters being the absorbed dose rate, the absorbed dose distribution, radiation quality. The environmental factors can be grouped as temperature, moisture content and oxygen concentration. SHRI at Vadodara has provided valuable experience regarding the design, operational parameters and economics of the process [6]. This paper addresses the issue of design optimization of the source assembly inside SHRI irradiator vessel thus improving the physical parameters. Better absorbed dose rates along with uniform dose distribution are the targets of this design optimization.

3. CALCULATION OF AVERAGE ABSORBED DOSE RATE

3.1 Cylindrical Shell Source with a Finite Length

The expression by Yamakoshi [12] for radiation dose rate distribution around a cylindrical shell source with a finite height has been used for the evaluation of dose rate. Dose rate at any point $p(r_d, \theta, h)$ is given as

$$D(r) = C_o \phi \quad (1)$$

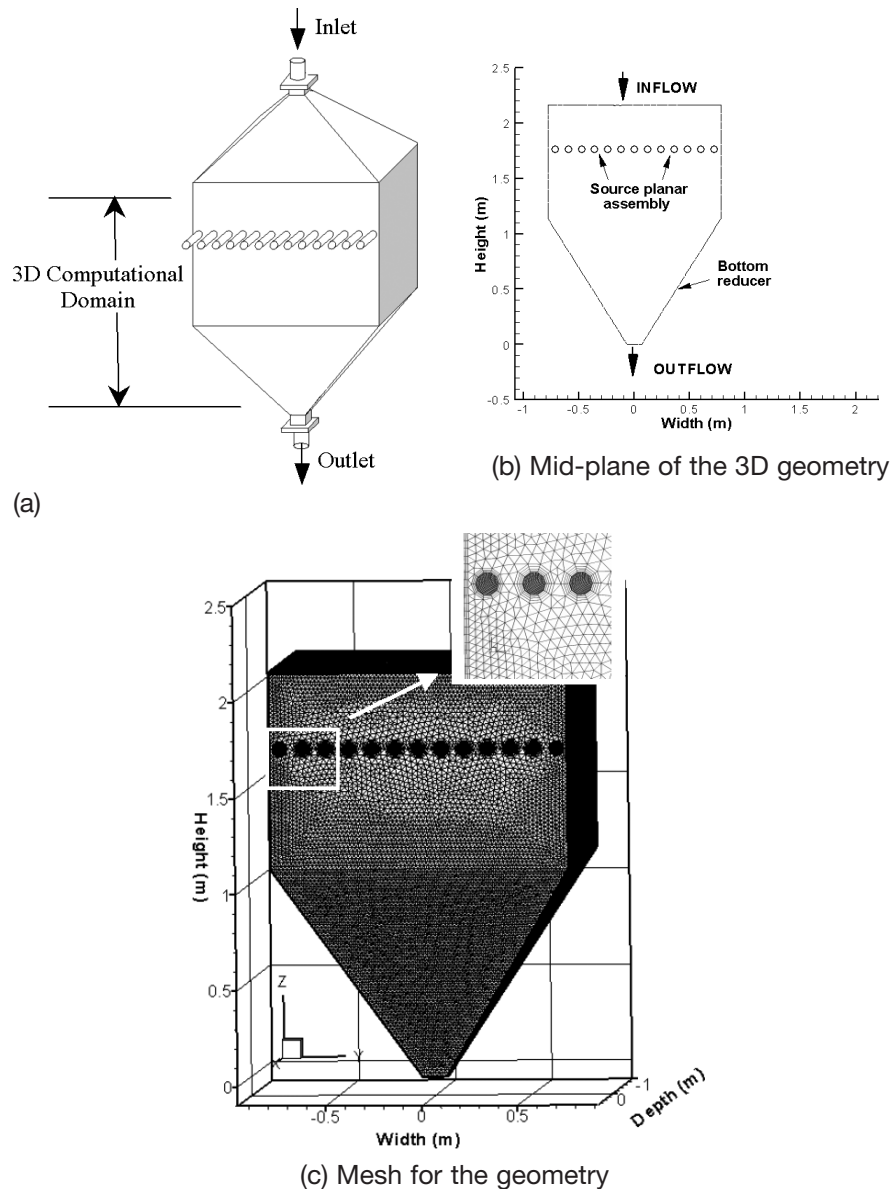


Figure 2. (a) Existing irradiation vessel geometry, (b) Mid-plane illustrating the gamma source planar assembly and (c) Mesh for the geometry in SHRI.

where C_o is the flux to dose rate conversion factor and

$$\phi = \frac{S_o H r_s}{\pi} \int_0^{\theta_c} \frac{(r_d \cos \theta - r_s)}{(r_d^2 + r_s^2 - 2r_d r_s \cos \theta) \cdot (r_d^2 + r_s^2 - 2r_d r_s \cos \theta + H^2)^{\frac{1}{2}}} d\theta \quad (2)$$

The description of the terms used in Eqn.(2) is shown in Fig. 3. Simpson's 1/3rd rule has been used in evaluating the integral.

3.1.1 Calculation of Time Averaged Dose Rate for Moving Medium

In our approach the basic idea is to use computational fluid dynamics (CFD) to simulate the movement of sewage sludge through the irradiation system and calculate their exposure time to ^{60}Co . This approach makes it possible to quickly determine the effectiveness of any proposed design. A CFD simulation provides fluid velocity, pressure and other appropriate variables throughout the computational domain.

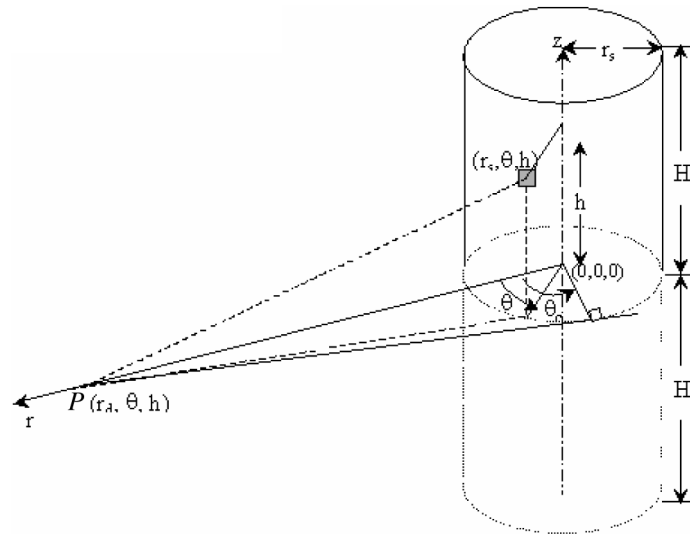


Figure 3. The calculation of dose rate for a cylindrical source of finite length.

The path taken by any sludge particle in the irradiator determines the amount of gamma radiation that it will be exposed to. The irradiator can then be designed to eliminate bypass, flow separation and dead zones that can result in reduction of irradiation time.

Let us define a few quantities.

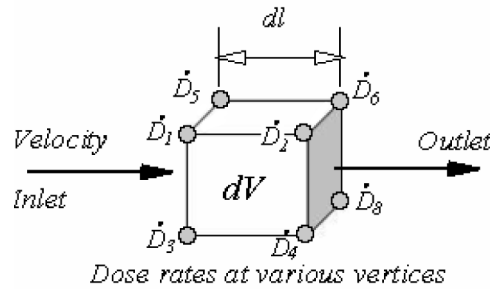


Figure 4. A typical fluid volume.

A fluid streamline with instantaneous absorbed dose rate, \dot{D}_i and velocity, v_i takes time $d\tau_i$ to traverse a length dl in a volume dV . It is shown in Fig. 4. Values of \dot{D}_i 's and v_i 's are available at the vertices of the fluid volume.

$$\text{Residence time of a particle along a streamline} = \int_{\text{inlet}}^{\text{outlet}} d\tau_i = \int_{\text{inlet}}^{\text{outlet}} \frac{dl}{v_i} \quad (3)$$

where limits of integral are the inlet and outlet of the irradiation vessel. The distribution of this quantity of various streamlines gives an approximate residence time distribution (RTD).

$$\text{Average absorbed dose rate for a fluid volume } dV \text{ in Fig. 4, } \dot{D}_r = \frac{\int_{\text{inlet}}^{\text{outlet}} \dot{D}_i dl}{\int_{\text{inlet}}^{\text{outlet}} dl} \quad (4)$$

$$\text{Volumetric absorbed dose rate, } \dot{D}_v = \frac{\int \dot{D}_r dV}{\int_V dV} \quad (5)$$

The distribution of this quantity is the volumetric absorbed dose rate distribution (VADRD). This distribution depends on the geometry of the irradiation vessel and location of radiation source under consideration.

The net dose absorbed D_i by a fluid particle in a volume dV will be governed by dose rate \dot{D}_i and velocity of the fluid particle while traversing distance dl from input to output of the volume with a residence time $d\tau$.

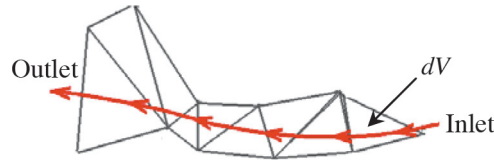


Figure 5. The Residence time for a streamline.

The local net dose absorbed D_i in a volume dV can be written as

$$D_i = \int_{inlet}^{outlet} \dot{D}_i d\tau_i = \int_{inlet}^{outlet} \frac{\dot{D}_i dl}{|v_i|} \tag{6}$$

$$\text{Local residence time in volume } dV, \tau_i = \int_{inlet}^{outlet} \frac{dl}{|v_i|} \tag{7}$$

$$\text{Time averaged absorbed dose rate for the whole domain, } \dot{D}_i = \frac{\int_V D_i dV}{\int_V \tau_i dV} \tag{8}$$

The numerator is the total dose ($Gy.m^3$) absorbed by all streamlines and denominator is the total time ($hr.m^3$) taken by all the streamlines in passes through the fluid volume. The distribution of this quantity is the time averaged absorbed dose rate distribution (TADRDR). This distribution depends on the fluid mechanical aspects of in the irradiation vessel. The parameters of fluid flow can be optimized, by improving TADRDR distribution.

One need not track individual particles but do a quick calculation for dose absorption. For example take a 2D case as in Fig. 6(a). The CFD solution gives us the values of velocity at vertices. Absorbed dose rate at the vertices has been calculated using Eqn. (1). The dose absorbed by the fluid entering this triangle and leaving has to travel a distance dl with an average velocity being v in time τ_i . Thus, the dose accumulated on passing this element in the volume dV is $\dot{D}_i \cdot \tau_i \cdot dV$. Thus the total absorbed dose in volume dV is obtained by summing up over number of elements, N and is $\sum_N \dot{D}_i \cdot \tau_i \cdot dV$. See Fig. 6(b) for tetragon.

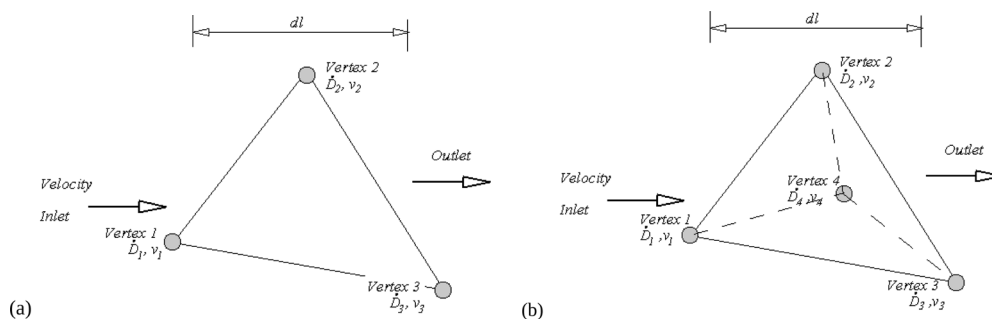


Figure 6. An illustration of (a) triangular (b) tetragonal element used in 2D and 3D analysis.

$$\text{Hence time averaged absorbed dose rate, } \dot{D}_t = \frac{\sum \dot{D}_i \tau_i dV}{\sum \tau_i dV} \quad (9)$$

Here all elements (N) of the grid would contribute to the streamline integration. The integration is performed over the whole domain of the fluid using the grid elements.

3.2 Validation of Average Absorbed Dose Rate

The experimental study by Benny *et al.* [8] used TL dosimetry for estimation of the average absorbed dose rate in the sewage sludge of SHRI and has reported a value of 0.7 ± 0.02 kGy/hr for 2.78 PBq loading of Cobalt source.

The Computational Fluid dynamics (CFD) simulation was performed for the irradiator vessel. Figure 2(a) shows the 3D computational domain used for the simulation. The mid-plane of the geometry is shown in Fig. 2(b) Figure 2(c) shows the mesh for the geometry. 3D geometry has been meshed with tetragons along with hexahedral boundary layers. The opensource CFD software OpenFOAM [13] has been used for solving the incompressible Navier Stokes. $k-\varepsilon$ turbulence model, with standard wall functions have been incorporated. The sewage sludge starts behaving like a plastic medium if the solids content is $>7\%$ by weight [3]. The solid content in the sludge dealt in this paper is 2% to 6%. So, Newtonian fluid dynamics with appropriate density correction has been used in these simulations. The boundary conditions of inflow and outflow were applied at the top and bottom of the computational domain of the irradiator.

The grid independence study was performed. A pressure drop of 359 Pa was obtained from inlet to outlet of the computational domain. The simulation produced a recirculation or dead zone inside the geometry below the source rod assembly. This recirculation or dead zone obtained has been earlier reported by Pant *et al.* [9,14] and Mahendra *et al.*[10].

Figure 7(a) shows the velocity contours within the zone around the planar source assembly. Each source being 60 mm in diameter are placed with a pitch of 120 mm. The sludge approaching the source assembly has a Reynolds number about 230 (calculated based on a single rod). CFD analysis revealed recirculation pockets below each source rod and a large recirculation zone just above the reducer section below the source assembly. The irradiator tapers in the bottom portion, which reduces the local, cross sectional area. The fluid in this zone accelerates and its effect is felt in the uniform cross section zone. Thus, higher velocities are obtained just above the tapered bottom section of the irradiator.

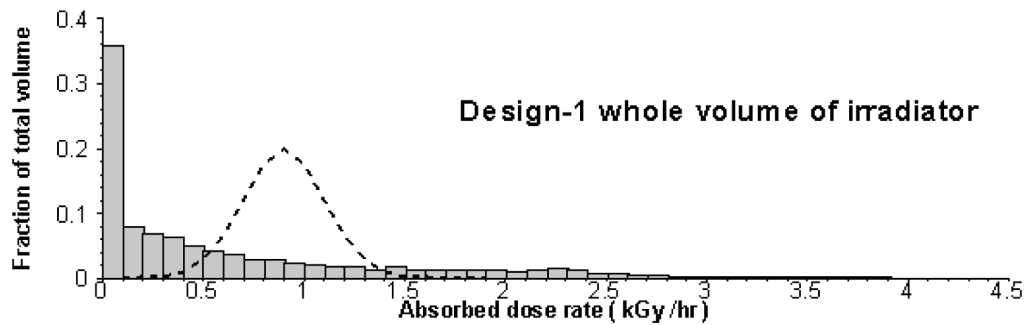
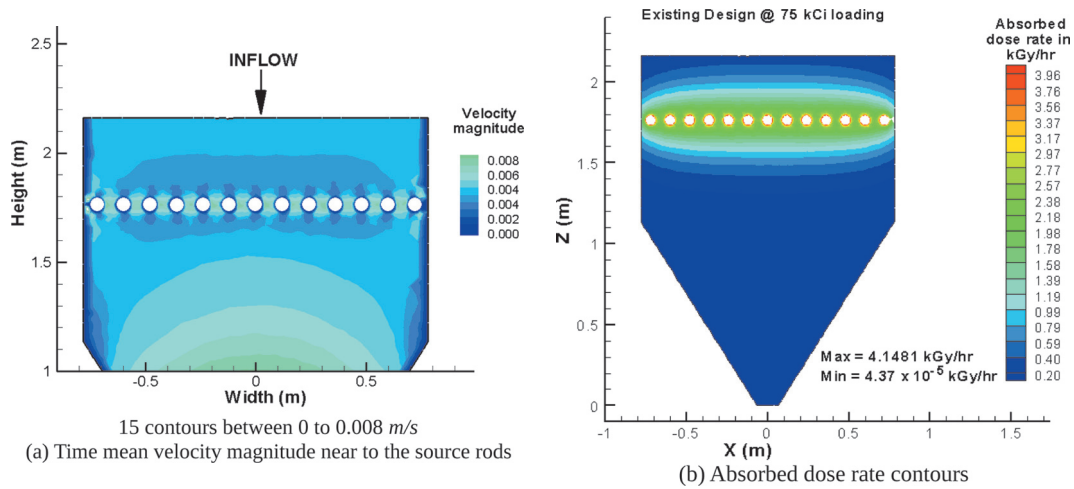
Figure 7(b) shows the contours obtained for absorbed dose rate calculated using Eqn. (1). There is high absorption of radiation in a zone near to the source assembly where as large portion of the irradiator is experiencing low absorbed dose rate. Figure 7(c) gives the volumetric absorbed dose rate distribution calculated using Eqn. (5) for the whole volume of irradiator. As evident from the distribution we find large portion of the irradiator with extremely low absorbed dose rate. The bottom portion of the irradiation vessel in form of a reducer constituting a sufficiently large volume was found contributing to low dose rate peak close to zero. This has been confirmed through Fig. 7(d) where the distribution was plotted after removing the portion of bottom reducer. The steep peak near zero dose rate was found to subside. Even though the reducer is contributing largely to low dose rate volume, it is required to have reducer so as to avoid sludge deposition.

The distribution in Fig. 7(d) still has a high fraction of volume absorbing < 0.5 kGy/hr of absorbed dose rate. There is a design constraint in SHRI to maintain about 390 mm of sludge above the topmost bank of gamma source rods. This ensures that radiation from the gamma source sufficiently decays inside the sludge before it reaches the top free surface of the sludge in the irradiator vessel. As expected this volume of irradiator experiences low absorbed dose rate. Thus, this portion of the volume contributes heavily to the dose rate below 0.5 kGy/hr.

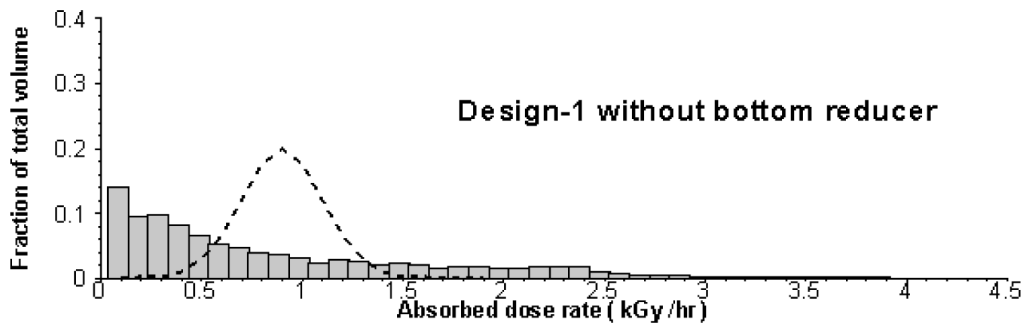
The dotted line in Fig 7(c) and 7(d) shows the expected target distribution. This was obtained using the following assumptions (1) the average absorbed dose rate targeted (*i.e.* 0.9 kGy/hr) was taken as mean (2) with a standard deviation of 0.2 kGy/hr. Unlike, the regular normal distribution here the sum of ordinates is equal to 1. The Fig. 7(c) shows a gap between the actual and expected absorbed dose rate distributions. This analysis shows that the geometry has good scope for design optimization to improve the absorbed dose rate distribution.

Table 1 shows the comparison between the experiment and the calculated value of average absorbed dose rate. Volumetric averaged absorbed dose rate is calculated using Eqn. (5) and time

averaged absorbed dose rate is calculated using Eqn. (9). Volume averaged absorbed dose rate underestimates the experimental average absorbed dose rate by 13%. Time averaged absorbed dose rate overestimates the experimental average absorbed dose rate by 16%. The experimental value is bounded between the two estimates.



(c) Volumetric absorbed dose rate distribution for whole volume of irradiator



(d) Volumetric absorbed dose rate distribution for irradiator without bottom reducer

Figure 7. The results of analysis of existing geometry (design-1) of SHRI {(a) to (d)}.

Table 1: Comparison of average absorbed dose rate estimation of SHRI

	Absorbed dose rate
Experimental value [8]	0.7 ± 0.02 kGy/hr
Volume averaged absorbed dose rate using Eqn.(5)	0.6099 kGy/hr
Time averaged absorbed dose rate using Eqn. (9)	0.8123 kGy/hr

4. NEW DESIGNS CONSIDERED

Based on the analysis carried out so far there was a need felt for a more optimum design. The following aspects were considered while converging at the new designs.

1. Distributing the source rod assembly into multiple levels would improve the VADRD in Fig 7(c) by making it more flat. So, there should be distribution of rods along axial direction. In order to minimize the radiation handling difficulties during loading and unloading phase, we propose to choose only such configurations, which are distributed in not more than 3 rows.
2. Solid blockage due to source rods in the irradiator vessel brings in resistance to flow. A decrease in solid blockage would decrease the pressure drop in the equipment. The existing case has a solid blockage of 50%. The new designs namely, design-2, design-3 and design-4 considered are having 50%, 34.6% and 34.6% solid blockage respectively.
3. The dose absorbed by a particle moving along a streamline will increase with the residence time of the streamline. Triangular pitch between two consecutive source rod assemblies increases the residence time appreciably. Triangular pitch ensures better mixing of sludge as it passes the irradiator. On contrary, when the tubes are in tandem (*i.e.* in square pitch), the tubes in the 2nd or/and 3rd row come in the wake of the tubes in 1st or/and 2nd row. This reduces the efficiency of absorbed dose rate distribution due to poor mixing although it reduced the pressure drop.

Three candidate design configurations considered for analysis have multiple planar source assemblies. The arrangement of the source rods in these planar assemblies gives new designs namely, design-2, design-3 and design-4. The new designs chosen for analysis are shown in Fig. 8.

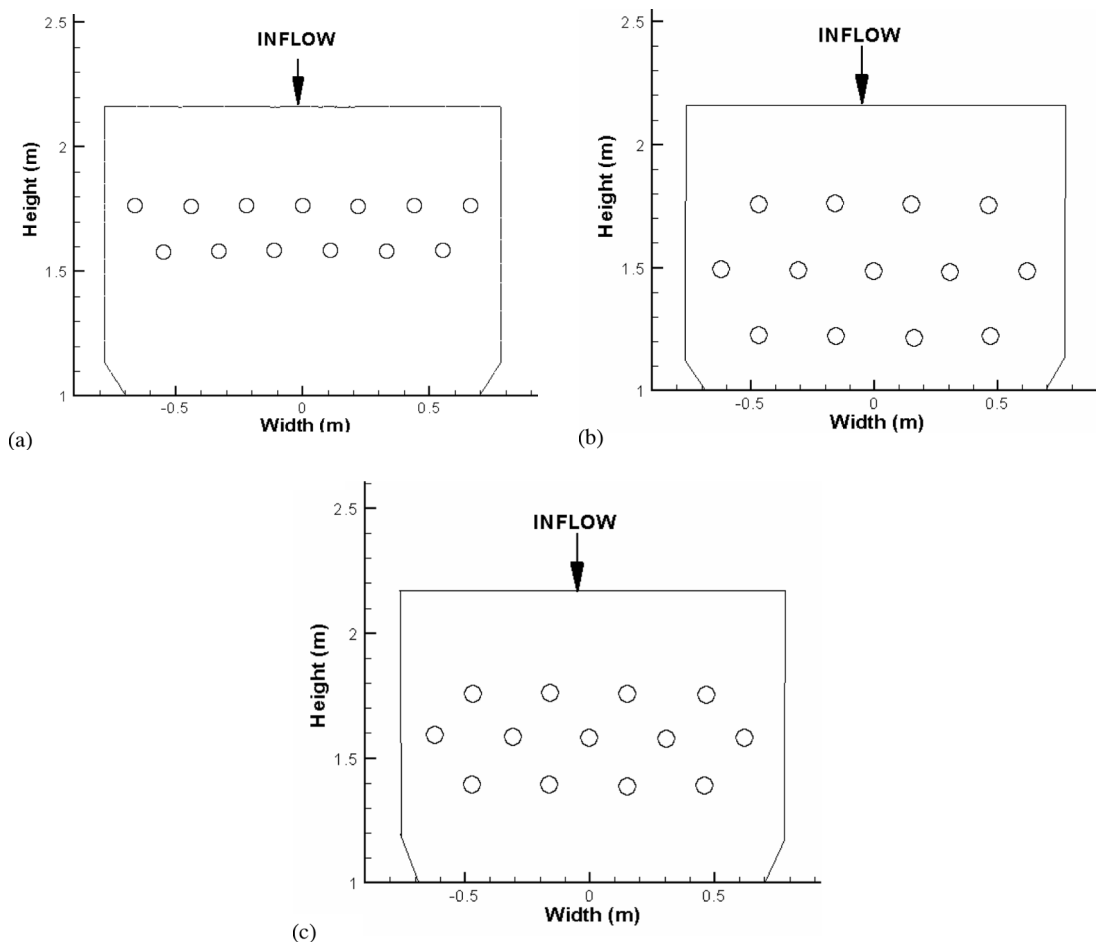


Figure 8. The cross-section view near the source assembly for (a) design-2, (b) design-3 and (c) design-4.

Details of these designs are depicted in Table 2. The design-2 is having only 2 planar assembly whereas design-3 and design-4 have 3 planar assemblies. The design-3 and design-4 have 1st and 3rd rows in square pitch (tubes in tandem), yet the distance between them ($\sim 9d$ and $\sim 6d$ respectively) is sufficient to minimize the wake effects. The problem at hand is a gravity driven flow situation, where the pressure loss is not of great concern.

Table 2: The details of source rods assemblies in the new designs

	Distance Between Centers of 2 Rods in a Plane	Distance Between 2 Consecutive Planes
Design-2	3.67d	3.03d
Design-3	5.17d	4.48d
Design-4	5.17d	3.03d

5. RESULTS AND DISCUSSION

The CFD simulations of design-2, design-3 and design-4 have revealed useful information of the configurations considered. Design-2 has a large recirculation or dead zone similar to design-1. CFD simulations of design-3 and design-4 do not reveal the presence of any large recirculation or dead zone inside the irradiator. The design-3 and design-4 have lower solid blockage. It causes two effects (a) reduces the velocity of fluid near the source assemblies, hence the residence time of the fluid increases and (b) reduces the pressure drop. The pressure drop is lowest for the design-3, followed by design-4 and design-2. Based on the CFD analysis design-3 and design-4 looks promising.

Figure 9(b), (d) and (f) show the time mean velocity magnitude contours obtained from CFD simulation. 15 contours are marked between the velocity magnitudes of 0 to 0.008m/s. It is clearly seen

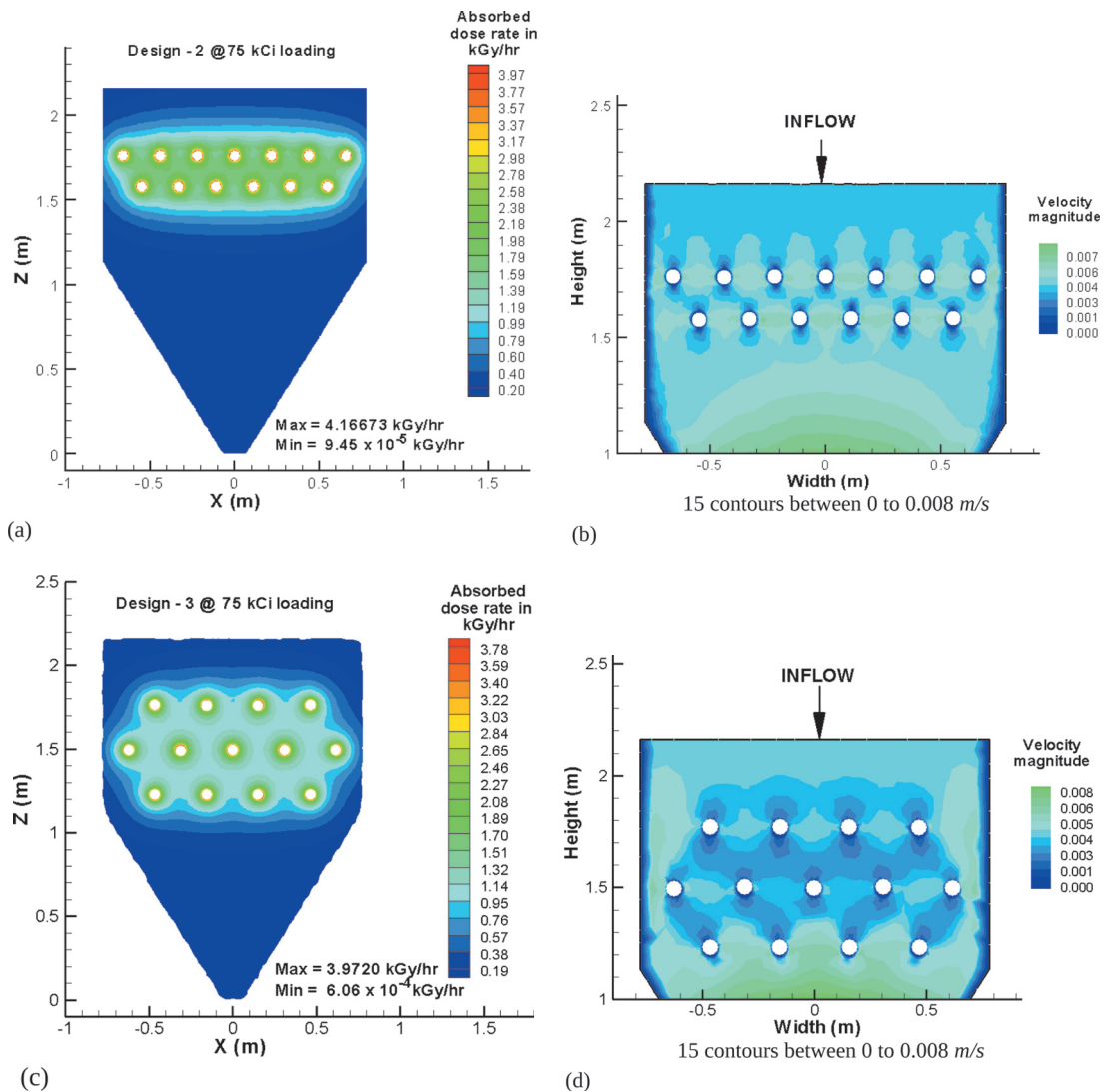


Figure 9. Estimated absorbed dose rate for (a) design-2, (c) design-3, (e) design-4 and time mean velocity magnitude for (b) design-2, (d) design-3, (f) design-4

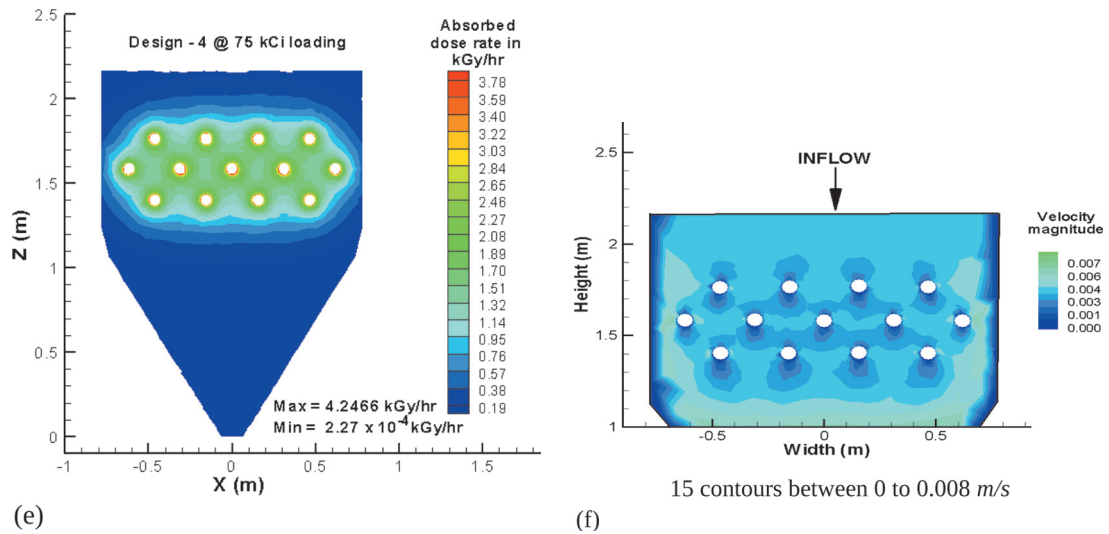


Figure 9. (Continue)

the wake affect is properly captured. Figure 9 (a), (c) and (e) show the absorbed dose rate in the irradiator vessel for the design-2, design-3 and design-4 respectively.

Table 3 gives a comparison of average absorbed dose rate between the four geometries considered. The radioactivity loading has been kept constant at 75.135 *kCi*. Design-2 has yielded a higher value of volume averaged absorbed dose rate than design-1. Design-3 and 4 have given higher values of absorbed dose rates. Thus design-4 is preferred as both the average absorbed dose rate estimates are higher.

Table 3: Comparison of absorbed dose rate for various designs considered

	Design-1	Design-2	Design-3	Design-4
Volume averaged absorbed dose rate using Eqn. (5) <i>kGy/hr</i>	0.610	0.648	0.681	0.690
Time averaged absorbed dose rate using Eqn. (9) <i>kGy/hr</i>	0.812	0.754	0.880	0.897
Pressure drop <i>Pa</i>	359	285	173	238

The volumetric absorbed dose rate distribution calculated using Eqn.(5) is plotted in Fig.10. Figures 10(a), (b) and (c) gives us the analysis for the Fig.'s 9(a),(c) and (e) respectively. Design-2 improves the distribution over design-1 yet it is far from the desired target distribution. Design-3 is very close to the desired target distribution whereas, design-4 deviates considerably from the target. From the VADR plots one would prefer design-3 among all the designs considered, as it is closer to the desired value. It should be noted that after irradiation the sludge is passed to a mixing tank and this repeated cycles of irradiation and mixing leads to uniformity in dose distribution. Thus in such a case time averaged dose rate and volume averaged dose rate become important dose parameters. Based on these two dose parameters design-4 is the recommended configuration for SHRI.

6. CONCLUSIONS

The new approach proposed to evaluate time averaged absorbed dose rate was over predicting the experimental findings by 16%. On contrary, the volume averaged absorbed dose rate approach was under predicting the average absorbed dose rate (experimental value) by 13%. In a way, the experimental finding has been bounded on both sides using the two approaches discussed in this paper. Volume averaged dose rate does not give a true picture of the absorbed dose rate as the residence time of the fluid element changes throughout the irradiator vessel. Whereas time averaged dose rate is based

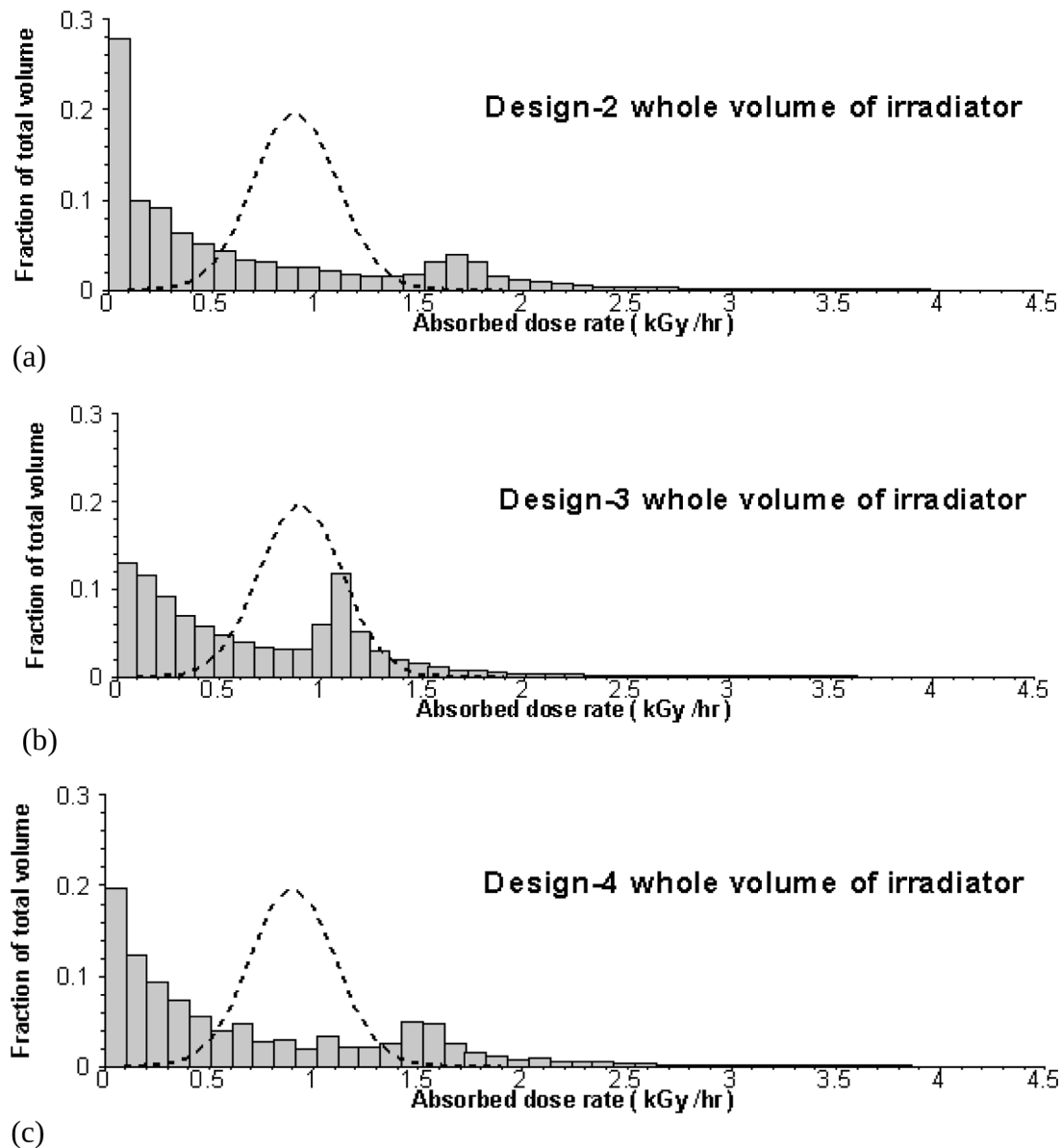


Figure 10. Volume averaged dose rate distribution for (a) design-2, (b) design-3 and (c) design-4.

on absorbed dose, thus it takes into account the residence time of the fluid element. Dose uniformity is also an important aspect apart from these two dose parameters.

Within the constraints of operation, the possible new designs were arrived at. The analysis over these designs showed that the design-3 and design-4 are better than design-1 based on the objective functions of time averaged dose rate, volume averaged dose rate and absorbed dose distribution. Design-4 even though with higher volume and time averaged absorbed dose rates than design-3, does not have a dose rate distribution, which peaks near its mean value.

Based on the absorbed dose rate distribution design-3 looks to be an optimum however, it has lower time averaged and volume averaged absorbed dose rate than design-3. On the other hand design-4 appears another optimum with higher time averaged and volume averaged absorbed dose rate although its distribution is worse than design-3. Since the uniformity of dose distribution is assured to a little extent by the use of circulation cycles consisting of irradiation followed by mixing. Consequently the geometry giving higher average absorbed dose rate is preferred than a geometry giving better absorbed dose distribution. Thus, in the present study design-4 is recommended.

7. ACKNOWLEDGEMENTS

Authors would like to thank Dr. S.Sabharwal, Shri M.R.Shah of SHRI facility Vadodara and Dr. H.J.Pant of Isotope Application Division of Bhabha Atomic Research Centre.

REFERENCES

1. Borrely S.I., Cruz A.C., Del Mastro N.L., Sampa M.H.O. and Somessari E.S., Radiation processing of sewage and sludge. A Review, *Progress in Nuclear Energy*, 1998, 33(No.1/2), 3–21.
2. BAO Borong, WU Minghong, History and prospects of irradiation treatment of sewage sludge, *Nuclear Science and Techniques*, Vol.10, (No.1),1999, 14–18.
3. Control of Pathogens and Vector Attraction in Sewage Sludge (Including Domestic Septage) Under 40 CFR Part 503, Environmental Regulations and Technology *Report No.EPA/625/R-92-013*, Revised October 1999, U.S. Environmental Protection Agency, Cincinnati, OH 45268, 1–181.
4. Iya, V.K. and Krishnamurty, K., Radiation treatment of sewage sludge in India, *Radiat. Phys. Chem.*, 1984, 24(1), 67–75.
5. Krishnamurty, K., Parametric relationships for gamma dose and irradiation homogeneity in a sewage sludge irradiator, *Radiat. Phys. Chem.*, 1986, 28, 381.
6. Lavale, D.S., Shah, M.R., Rawat, K.P. and George, J.R., Sewage sludge irradiators, *IAEA-TECDOC-1023*, 1998, Vienna, Austria.
7. Benny P.G., B.C. Bhatt, High-level gamma dosimetry using photo transferred thermoluminescence in quartz, *Applied Radiation and Isotopes*, 2002, 56, 891–894.
8. Benny P.G., B.C.Bhatt and M.R. Shah, TL dosimetry using extracted and cleaned sand to measure gamma-ray dose rate at a liquid sewage sludge irradiation facility, *Radiat. Phys. Chem.* 1997, 49(No. 3), 377–381.
9. Pant H. J., Thýn J., Zitný.R and Bhatt B.C., Radioisotope Tracer Study in a Sludge Hygienization Research Irradiator (SHRI), *Appl. Radiat. Isot.*, 2001, 54, (Number 1), 1–10
10. Mahendra A.K., Sanyal A., Gouthaman G., Simulation and optimization of sludge hygienization research irradiator, *Proceedings of International conference on current trends in industrial and applied mathematics*, Vadodara, 16–18 January, 2007.
11. Suess A., Potential harmful effects on agricultural environments of sewage sludge utilization as a fertilizer. In *Proceedings of consultants meetings on Sewage sludge and wastewater for use in agriculture*, 1977, Oct 1997, 159–167
12. Yamakoshi H., A simple expression for radiation dose rate distributions around cylindrical shell source with a finite height, *Nucl. Sci and Engg.*, 1984, 88, 110–122.
13. OpenFOAM, The Open Source CFD Toolbox, *User Guide, Version 1.6*, 24th July 2009, 1–203.
14. Pant H.J., Patwardhan, A., Mahendra, A.K., Ranade, V.V., Validation of CFD models and integration of CFD-RTD methods for industrial process visualization and optimization, *IAEA-TECDOC 1412*, 2004, 119.